Intermediate range O–O correlations in supercooled water down to 235 K

Harshad Pathak (iD), Alexander Späh (iD), Kyung Hwan Kim, Ifigeneia Tsironi, Daniel Mariedahl, Maria Blanco, Simo Huotari, Veijo Honkimäki, and Anders Nilsson

View Online   Export Citation   CrossMark

ARTICLES YOU MAY BE INTERESTED IN

The Journal of Chemical Physics

Submit Today

The Emerging Investigators Special Collection and Awards
Recognizing the excellent work of early career researchers!

AIP Publishing

Intermediate range O–O correlations in supercooled water down to 235 K

View Online   Export Citation   CrossMark

Harshad Pathak,[1,a] (ID) Alexander Späh,[1] (ID) Kyung Hwan Kim,[1] Ifigeneia Tsironi,[1] Daniel Mariedahl,[1] Maria Blanco,[2] Simo Huotari,[3] Veijo Honkimäki,[2] and Anders Nilsson[1]

AFFILIATIONS

[1] Department of Physics, AlbaNova University Center, Stockholm University, SE-10691 Stockholm, Sweden

[2] European Synchrotron Radiation Facility, 71 Avenue des Martyrs, 38000 Grenoble, France

[3] Department of Physics, University of Helsinki, FI-00014 Helsinki, Finland

Note: This paper is part of a JCP Special Topic on Chemical Physics of Supercooled Water.
[a] Author to whom correspondence should be addressed: harshad.pathak@fysik.su.se

ABSTRACT

Wide angle x-ray scattering of supercooled water down to 234.8 K was studied using high energy x rays at the European Synchrotron Radiation Facility. The oxygen-oxygen pair distribution function (PDF) was calculated from the scattering pattern out to the 5th peak at an intermolecular distance, $r \approx 11$ Å. We observe that the 4th peak and the 5th peak in the PDF increase in height upon supercooling. We also observe that the 4th peak position (r_4) shifts to shorter distances upon supercooling consistent with previous studies, but we see a more rapid change at the lowest temperature. The running oxygen-oxygen coordination number is calculated for 5 different temperatures, and an isosbestic point at $r_{iso} = 3.31 \pm 0.05$ Å was found corresponding to a coordination number of 4.39 ± 0.15. The comparison of the PDF of the coldest water with that of amorphous ice shows distinct differences. We propose that there are 5-member pentamer rings in low density liquid-like structures giving rise to the sharp correlations at $r \approx 9$ Å and $r \approx 11$ Å.

I. INTRODUCTION

Water is one of the most important liquids for various biological and geological processes in nature. Its importance relates to its unique properties, which are different than those of normal liquids,[1] and a lot of effort has been made to understand these peculiar properties.[2–6] An interesting anomaly is that water becomes more compressible on cooling from 319 K onwards and thereby exhibits a distinct behavior compared to other liquids where compressibility usually decreases on cooling. This is the temperature range where many important biological activities take place. What is particularly interesting is that the compressibility diverges in the supercooled regime[7] and eventually reaches a maximum[8] at 229 K. This divergence is accompanied by a rapid growth of tetrahedral structures.[8,9] Our aim in this study is to explore what are the changes to the intermediate-range structure taking place at the supercooled conditions correlated with the growth of tetrahedral structures and diverging compressibility.

A water model that can elucidate the anomalous properties is based on a hypothesis that water can exist transiently in two distinct local environments—low-density liquid (LDL) and high-density liquid (HDL).[10–16] These local environments when under pressure and low temperature have been proposed to lead to macroscopic liquid phases with a phase boundary that ends with a critical point at a positive pressure and as such being consistent with experimental data.[4,6,8,17] LDL consists of water molecules that upon decreasing temperature form tetrahedral structures which are favored by enthalpy, whereas HDL consists of molecules where the tetrahedral structure has collapsed and is entropically favored, resulting in higher density.[18] The latter is dominating at ambient and elevated temperatures.[4]

Small angle x-ray scattering (SAXS) experiments probe instantaneous density heterogeneities in liquids and show that such heterogeneities increase upon cooling water[8,19] from ambient conditions into the supercooled regime. However, SAXS alone is insufficient to determine the detailed structural changes causing these density fluctuations. There have been numerous x-ray scattering measurements to derive the two-body oxygen–oxygen (O–O) pair distribution functions (PDF) that are essential to obtain information on the long-range structure of water.[20–28] Recent advances in bright x-ray facilities have made it possible to use high-energy photons where scattering data can be collected on large area detectors,[27,29] enabling a large measurement range of the momentum transfer vector, Q. A benchmark of the O–O PDF[27] of liquid water at ambient temperature has shown that a Q-range of at least 18 Å^{-1} is required for accurate determination of the PDF, in particular, for the height and narrowness of the first shell.

The intermediate range O–O PDF was first measured by Yokoyama et al.,[25] generating reliable data at 258 K, whereas at higher temperatures the data were too noisy. Correlations at 8.8 Å and 10.8 Å, corresponding to the 4th and 5th shells, were detected at 258 K, and from comparison with various ice forms, it was proposed that these are connected to the formation of clathratelike structures in supercooled water making up pentamer rings. Higher quality data for ambient and hot water were obtained by Huang et al.[30] where the 10.8 Å correlation diminished and a shift in the 4th shell to 9.5 Å at 340 K was observed. The experimental data were compared with simulations from the TIP4P/2005 water model.[31] There was a good agreement between the measurements and the simulations at O–O correlations beyond the 3rd shell allowing for in-depth analysis of the simulation results. The water molecules in the simulations were analyzed into structured LDL-like configurations and disordered HDL-like environments based on their local structure index[32,33] (LSI). The O–O PDF of water was separated into these two types of structural environments with LDL-like and HDL-like structures dominating at low and high temperatures, respectively.

Schlesinger et al.[34] analyzed the temperature dependent intermediate-range O–O correlations in the temperature range of 254–348 K based on high Q experimental data by Skinner et al.[35] as well as simulations from the TIP4P/2005 water model[31] with a similar analysis using LSI as in the study of Huang et al.[30] Here, more detailed information could be obtained over a larger temperature range. We note that indeed these correlations become extremely weak at distances beyond the 3rd shell. The study showed that the 5th peak in the PDF is absent at temperatures above 319 K and starts to appear at temperatures colder than 319 K at r5 ≈ 11 Å, coinciding closely with the temperature of the compressibility minimum, and was proposed to be related to the increase in the compressibility at decreasing temperature.[4] This 5th peak is associated with water's LDL-like structures and, subsequently, increasing tetrahedrality that generate large regions allowing correlation distances of 11 Å.[4,28,30,36] The 4th peak is located at r4 ≈ 9 Å at a high temperature and shifts to shorter distances with an accompanying peak height increase upon cooling below 260 K. The 4th peak location is sensitive to the relative balance of the HDL-like and LDL-like local structures, and since LDL-like structures have the correlations at shorter distances as compared to the HDL-like structures, the peak shifts to lower values of r upon cooling. For the PDF of a Lennard-Jones type of simple liquid, there is a smooth decrease in peak height at increasing distances.[37] However, in the case of water at temperatures higher than 254 K, we see that the 5th peak height is higher than the 4th peak height,[34,35] indicative of an anomalous liquid with overlapping HDL-like and LDL-like correlations. The O–O PDF for low-density amorphous ice (LDA) is much similar to hexagonal ice for the first and second peak locations.[38] The peak height for the second peak is much higher for crystalline ice because of a well-defined crystal structure. For higher values of r, they show considerable disagreement, indicating that the longer distance structure is distinctly different.

The O–O PDF correlations for water have been measured down to 254 K using acoustically levitated droplets[35] and down to 244 K using a glass capillary.[28] Experimental advances in the supercooling of water microdroplets, in a containerless environment, down to 227 K that can overcome homogeneous ice nucleation have recently become possible.[8,9] Here, we use a similar experimental setup[8] at a synchrotron radiation facility to measure x-ray scattering to high Q of micrometer sized droplets. The temperature range in these measurements at a synchrotron radiation facility is limited in comparison with an x-ray free electron laser (XFEL) since the exposure time is of the order of seconds to get sufficient statistics as compared to single-shot detection (in the order of 50 fs) at XFEL facilities. This exposure time determines the lowest temperature that we can measure without significant Bragg spots from crystalline ice. Here, we present the results of a wide-angle x-ray scattering (WAXS) experiments of liquid water down to 234.8 K at the European Synchrotron Radiation Facility (ESRF) where we extract the O–O PDF accurately beyond the 5th shell at r ≈ 11 Å.

II. MATERIALS AND METHODS

A. Experiments

Wide angle x-ray scattering (WAXS) of supercooled water with high-energy x rays was measured at 5 different temperatures ranging from 264 K to 234.8 K at beamline ID31 at the European Synchrotron Radiation Facility (ESRF). The x-ray energy was 67.95 keV with an energy bandwidth of 0.2 keV. The beam size was 5 μm (horizontal) by 20 μm (vertical) with a sample to detector distance of 163 mm. We used the Hybrid photon counting PILATUS3 X CdTe 2M detector, which allows single photon counting where each pixel is virtually an independent x-ray detector.[39] The pixel size was 172 μm, and the number of pixels were 1475 (horizontal) by 1679 (vertical). This detector negates dark current as a source of detector noise and enables high quality data.[40] Milli-Q water was used to produce a droplet train in situ with two different diameters (d$_{drop}$)— 40 μm for higher temperatures and 20 μm for our coldest temperatures of 240.9 K and 234.8 K. These droplets were cooled by evaporative cooling in a vacuum chamber, and droplet temperatures were estimated using a Knudsen theory of evaporative cooling[41] which has been tested for validity by both experiments[42] and simulations.[43] The details of the experimental setup are given in Ref. 9. We compare our scattering data with those of Skinner et al.[35] and Benmore et al.[28]

B. Analysis

The intensity as a function of Q to a maximum value (Q$_{max}$) = 21.6 Å^{-1} was measured with a Q-resolution of 0.029 Å^{-1}. However,

the data at high Q from 18.8 Å^{-1} (13.8 Å^{-1} for smallest droplets) onwards are noisy and therefore were cut off at Q$_{max}$ < 21.6 Å^{-1}. The measured signal is processed using the fit-2d program[44] which incorporates standard polarization and geometric corrections. The integrated signal is smoothened by a Savitzky-Golay filter with a window length of 0.5 Å^{-1}, improving the noise level without any significant distortion.[45]

The goal was to extract the differential cross section, normalized per molecule [$I(Q)$], as described in detail in Ref. 29. The background was measured by moving the droplet train away from the x-ray path and was directly subtracted from the detected water signal. This direct subtraction is acceptable[29] since there is more than 99.9% transmission of the high energy x rays from the micrometer sized droplets to the detector. For some detector images of our coldest temperatures, we observe diffraction peaks from crystalline ice and these are excluded from the data analysis. Multiple scattering and fluorescence are negligible at 67.95 keV for 20–40 μm thin water samples. The angular dependence detector attenuation is calculated for the 1 mm thick CdTe detector material. The space between the sample and the detector is referred to as a "filter." It consists of three parts—a 1 mm aluminum plate protecting the detector, a 125 μm Kapton (polyimide) window to separate the

vacuum chamber from the atmosphere, and 75 mm air. The combined attenuation from these materials is 7% with the majority coming from the aluminum plate. The oblique incidence correction from the detector and the filter is calculated resulting in a multiplicative correction.[29] The Compton scattering signal is calculated for water using quantum mechanical calculations[46] and corrected for the energy dependence and relativistic effects.[29] The inelastic signal dominates over the elastic signal at Q > 5 Å^{-1} and forms more than 90% of the signal at Q > 19 Å^{-1}. We therefore limited the Q$_{max}$ to 18.8–19.2 Å^{-1} for the 40 μm and 13.8–16.3 Å^{-1} for the 20 μm droplets.

The resulting $I(Q)$ is derived after the multiplicative correction (angular dependence of attenuation due to the detector and filters) and subtraction of the Compton scattering. The molecular structure factor [$S_{mol}(Q)$] is obtained from $I(Q)$ by the following equation:[27]

$$S_{mol}(Q) - 1 = \frac{I(Q) - FF(Q)}{WF(Q)}, \qquad (1)$$

where FF(Q) is the molecular form factor obtained from the quantum mechanical calculations of Wang *et al.*[46] and WF(Q) is the
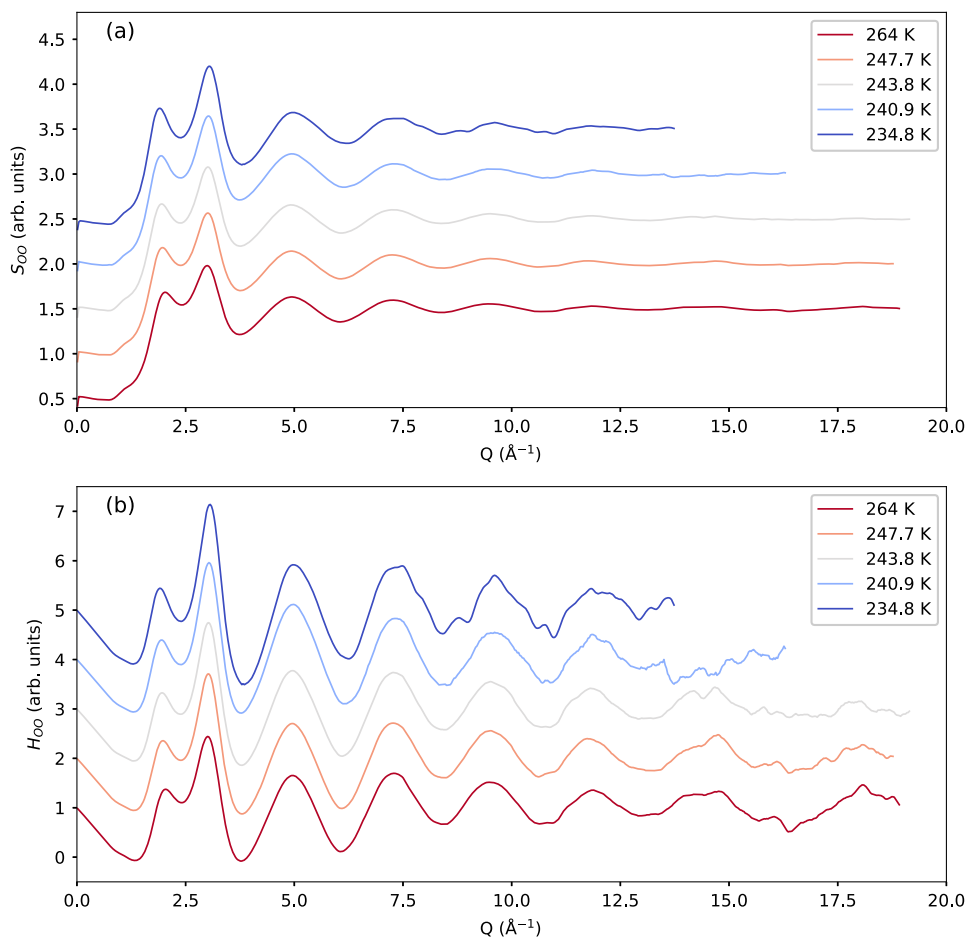

FIG. 1. S$_{OO}$(Q) and H$_{OO}$(Q) = Q × [S$_{OO}$(Q)−1] for different temperatures. H$_{OO}$(Q) is shown to emphasize the oscillations. The data are offset from each other for clarity. The data for high temperatures were measured with a droplet diameter of 40 μm, and 240.9 K and 234.8 K were measured with a droplet diameter of 20 μm.

weighting function given by

$$WF(Q) = f_O(Q)^2 + 4f_O(Q)f_H(Q) + 4f_H(Q)^2, \quad (2)$$

where $f_O(Q)$ and $f_H(Q)$ are the modified atomic form factors for oxygen and hydrogen, respectively, which were calculated from the atomic form factor and charge redistribution within the water molecule.[23] $S_{mol}(Q)$ consists of contributions from partial structure factors—the O–O, O–H, and H–H contributions. The H–H contribution[47] is less than 1% and is neglected. The O–H contribution needs to be subtracted, and here, an average of neutron scattering experiments[48] and molecular dynamics (MD) simulations was used.[31,49] O–H contribution varies from around 20% of the elastic signal at low Q and decreases to 2% Q ≈ 20 Å^{-1}. The temperature dependence of the O–H contribution is obtained from TIP4P/2005 simulations.[31] Neutron scattering experiments[35] on D_2O from 277 K to 348 K confirm that dS_{OH}/dT estimated from TIP4P/2005 is a reasonable approximation of the experimental data. The final O–O contribution (S_{OO}) to $S_{mol}(Q)$ is subsequently isolated after accounting for the O–H contribution and is illustrated in Fig. 1.

$S_{OO}(Q)$ is then used to extract the oxygen–oxygen pair distribution function (PDF), $g_{OO}(r)$, using a sine Fourier transform given by Eq. (3), where ρ is the number density of oxygen atoms,

$$g_{OO}(r) = 1 + \frac{1}{2\pi^2 \rho r} \sum_{Q=0}^{Q_{max}} Q \times (S_{OO}(Q) - 1) \times \sin(Qr) \times M(Q, \Delta r) dQ. \quad (3)$$

$M(Q, \Delta r) = \sin(Q\Delta r)/Q\Delta r$ is a Lorch function[50] used to reduce the unphysical oscillations in $g_{OO}(r)$, which have a period of $2\pi/Qmax$. There are different ways in which r-dependent averaging width, Δr, can be calculated.[27,35] The expression for Δr used here suppresses the unphysical oscillations except in the vicinity of first peak of $g_{OO}(r)$ and is similar to that used by Skinner $et\ al.$[35] and is given by

$$\Delta(r) = a\left(1 - \exp\left(-2.77\left(\frac{r - r_1}{\omega_1}\right)^2\right)\right) + a\left(\frac{1}{2} + \frac{1}{\pi}\arctan\left(\frac{r - \omega_2}{\omega_2/2\pi}\right)\right)\sqrt{r}. \quad (4)$$

The constants used are ω_1 = 0.5 Å, r_1 = 2.8 Å, and ω_2 = 12 Å.

III. RESULTS AND DISCUSSION

A. O–O pair distribution functions

The resulting O–O PDF $g_{OO}(r)$ for all the different temperatures are illustrated in Fig. 2. Figure 2(a) shows that the first three shells in $g_{OO}(r)$ increase with decreasing temperature. The features at r < 2.3 Å are artifacts due to truncation error from the Fourier transform and do not represent any real physical features.[51] The first shell peak height at r ≈ 2.8 Å increases on cooling and is expected based on previous results,[9,30,35] which have shown that the peak broadens asymmetrically toward longer distances on increasing temperature. This is due to transformation of tetrahedral structures of LDL-like configurations to the more disordered HDL configurations, where an increasing amount of water molecules occupies the interstitial space between the first and the

second shell, but also more disordered in the first shell within HDL configuration leading to additional broadening.[4] The increase in peak height of the second shell at r ≈ 4.5 Å is much more pronounced and is an indication of increased population of LDL-like molecules in tetrahedral configurations upon cooling.[9,17,28,30,35] Further analysis and comparison with MD simulations are discussed elsewhere.[52]

Next, we are interested in the intermediate range with a focus on the 4th and 5th shells located at r_4 ≈ 9 Å and r_5 ≈ 11 Å, respectively. The correlations at distances beyond that have artifacts from the Fourier transform. We use a Gaussian filter to smoothen the data where each value is an average of the points in the neighborhood weighted by a Gaussian function. In this study, we choose to focus on qualitative data analysis where trends in $g_{OO}(r)$ with respect to temperature are emphasized. Hence, we choose a broad Gaussian peak with a peak width (2σ) of 0.48 Å. This width is chosen to smoothen over the oscillations in $g_{OO}(r)$ which have a period of $2\pi/Qmax$ and are not completely removed by the use of Lorch function. Figure 2(b) illustrates this smoothened $g_{OO}(r)$.

We see from Fig. 2(b) that the 4th and 5th peak heights (g_4 and g_5, respectively) increase on decreasing temperature. The 4th peak shifts to shorter distances and becomes sharper on supercooling. Previous work[30,34] has shown that more LDL-like local environments result in the sharpening and shifting of the peak to shorter distances upon supercooling down to 254 K, and here, we see this to continue further at lower temperatures. At 234.8 K, we observe that g_4 increases and becomes higher than g_5 as expected for a simple liquid[37] with thermal fluctuations around an average structural configuration.[4,30,35] Since the temperature of the Widom line has been determined to 229 K,[8] we expect that LDL-like configurations will still be below 50% at 234.8 K. The reason for observing mostly LDL-like configurations at 234.8 K for g_4 and g_5 could imply that the LDL-like structure has become long-range ordered to dominate the O–O PDF in comparison with the HDL-like configurations. The latter are more disordered and thereby shows less correlations with distinct peaks at long distances.

B. Peak positions

A more detailed look at the peak position of the 4th and 5th shell (r_4 and r_5, respectively) with respect to temperature is shown in Fig. 3. The peak position is calculated by taking the numerical derivative with respect to r, $\Delta g_{OO}(r)/\Delta r$, and is fitted with a straight line around the vicinity of the peak, and the value of r when the line crosses zero gives the peak position. For comparison, we also include the data from the work of Skinner $et\ al.$[35] and Benmore $et\ al.$[28] with the same smoothening parameters as in the current study. We see from Fig. 3(a) that r_4 shifts to lower r upon cooling. The effect is already clearly seen in Fig. 2(b). This result is consistent with previous studies where LDL-like local environments result in r_4 shift[30,34] to shorter distances. We note that there is a more accelerated change in r_4 at temperatures below 250 K. Figure 4(b) shows the position of the 5th peak (r_5) for comparison where at higher temperatures, r_5 is shifted toward longer distances, suggesting an opposite trend as compared to r_4. At temperatures ≈250 K, this trend flattens out, and then, we observe r_5 only shifting marginally toward shorter distances at the lowest temperatures. We recalculate the O–O PDF with a near-identical Q_{max} of 13.6–13.8 Å^{-1} corresponding to the
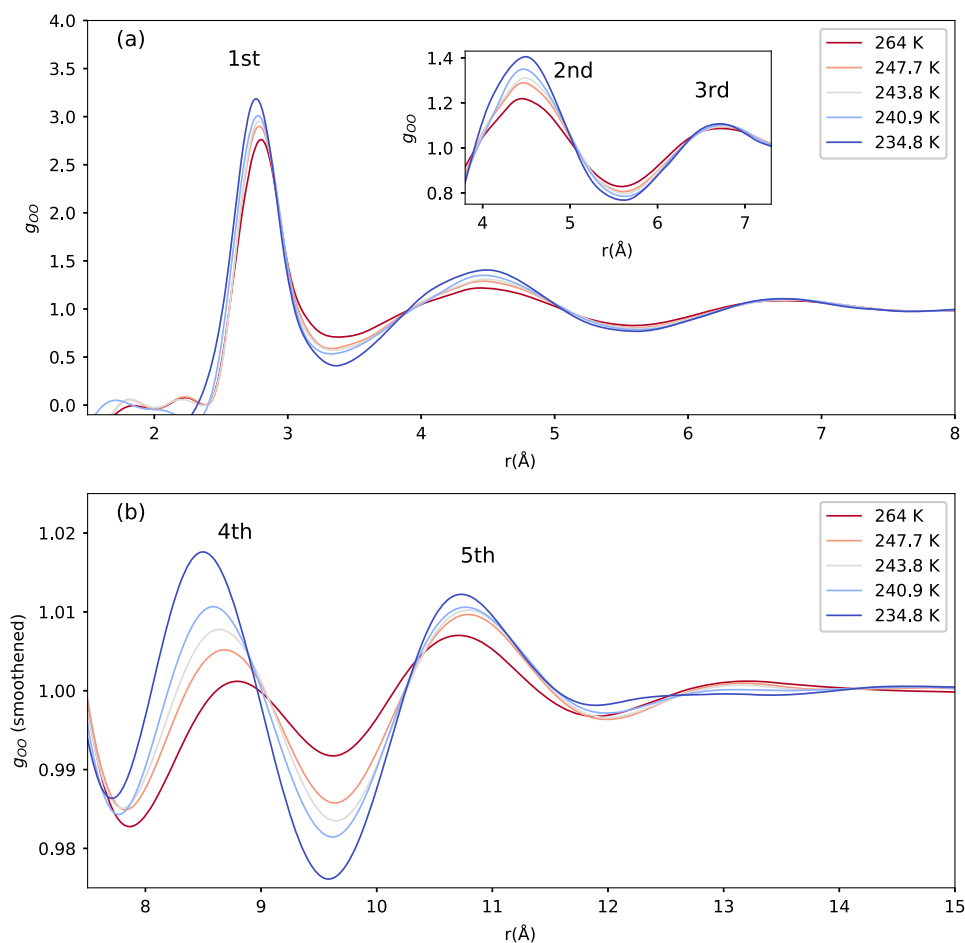
FIG. 2. The PDF, $g_{OO}(r)$, for different temperatures. (a) The first shells with a magnified inset of the second and third shells. (b) The intermediate-range where the data have been smoothened using a Gaussian function with a width (2σ) of 0.48 Å. Note the difference of scale in $g_{OO}(r)$ between the plots in (a) and (b).

nearest node [where $S_{OO}(Q)$ crosses zero] and show the results in the supplementary material. We see that there are small changes in the O–O PDF, but the peak positions are relatively unchanged. We also see a similar insensitivity of the peak positions to any error in $dS_{OH}(Q)/dT$.

C. Running O–O coordination number

It was demonstrated in the work of Skinner *et al.*[35] that there is an isosbestic point over a temperature range of 254 K–366 K at 3.30 ± 0.05 Å in the running O–O coordination, representing the integral of the pair distribution as a function of cutoff distance. Recently, this was also extended down to 244 K with an isosbestic point at 3.26 Å.[28] Figure 4 depicts the running O–O coordination number (n_{OO}) for water in the current study for temperatures between 234.8 and 264 K. We observe that there is indeed an isosbestic point at r_{iso} = 3.31 ± 0.05 Å, being close to the previous studies at higher temperatures. We also observe a n_{OO} of 4.39 ± 0.15 which is similar to 4.3 ± 0.2 in Ref. 35.

The implication of these results is that there is an isosbestic point with a constant running coordination number from 234.8 K

to 366 K, which is a large temperature interval. Although the PDF of water undergoes large changes as a function of temperature, the first coordination shell represented by the isosbestic points at 3.3 Å is constant. The consequence of this observation is that when the liquid rearranges with less coordination at 2.8 Å at higher temperatures, these molecules shift only to slightly longer distances with the 3.3 Å cut off distance. In the picture of conversion of HDL-like to LDL-like configurations, the number of molecules stays constant within the distance of the isosbestic point, and they do not move in or out of this first shell. We can envision that as LDL-like molecules, with 4-coordination at around 2.8 Å, convert to HDL-like configurations, some of the strongly bound molecules move to longer distances around 3.0–3.3 Å but are still regarded to be within the first shell and part of the 4-coordination.[4,53] The interstitials that appear in the HDL-like environment originate from the collapsed 2nd shell at 4.5 Å in LDL-like configurations upon heating and appear at distances longer than 3.3 Å. The existence of the isosbestic point over such a large temperature range therefore indicates that the rearrangements of molecules in terms of hydrogen bonding angles and distances appear separately within each shell defined as below or above 3.3 Å.
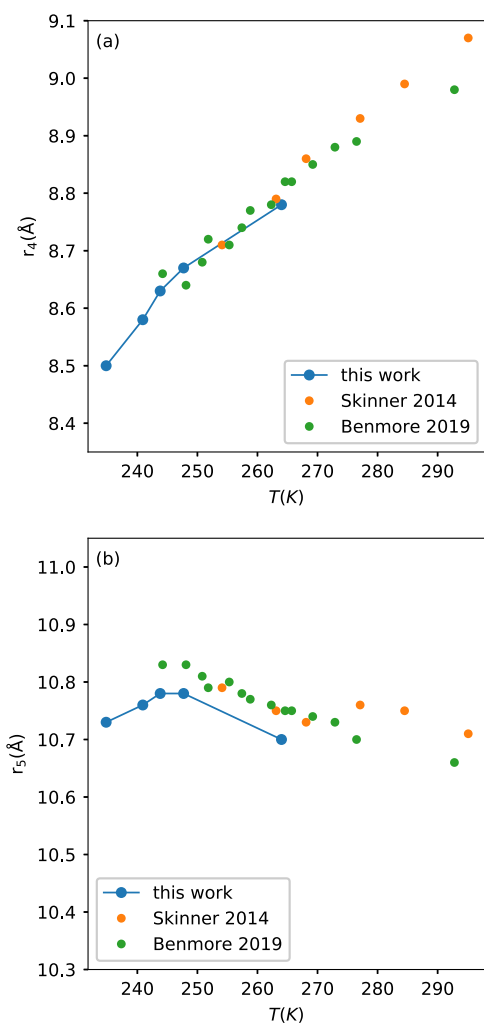
FIG. 3. (a) Peak location of the 4th peak of $g_{OO}(r)$ denoted by r_4. (b) Peak location of the 5th peak of $g_{OO}(r)$ denoted by r_5. "Skinner 2014" refers to Ref. 35 and "Benmore 2019" refers to Ref. 28.

FIG. 4. The oxygen–oxygen running coordination number (n_{OO}) for water. The region where we see an isosbestic point is shaded in gray.

D. Comparison with LDA

In order to gain more insights about the 4th and 5th shells in deeply supercooled water, we compare with low density amorphous ice[38] (LDA) which is hypothesized to be a glassy state of water[2] and, thereby, thermodynamically continuous with the liquid state.[2] The data for hexagonal ice are calculated from their crystal lattice parameters and, additionally, disorder was introduced by random displacements of approximately 0.08 Å, and the details of this approach are reported in Ref. 38. The 1st and 2nd shells show good agreement between water at 234.8 K, LDA, and hexagonal ice, as illustrated in Fig. 5. We note already a difference in the 3rd shell where water has more correlations at shorter distances than LDA. This is also present at higher temperatures[35] and consistent with the fact that HDL-like structures are not present in LDA accounting for this difference. Here, we assume based on the previous discussion that the O–O intermediate range correlations at the lowest
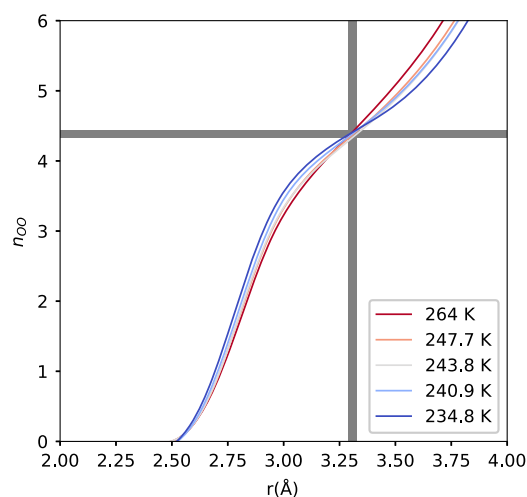
temperature are dominated by LDL-like configurations. We see that for the 4th shell, the liquid peak is narrower than that in LDA, which also has a weak shoulder toward lower distances. The contrast is even more pronounced in the 5th shell where water shows a narrow peak and at a significantly shorter distance at 10.7 Å than LDA, which instead has a broad plateau between 11 and 12 Å. Here, we see clear evidence that the LDA structure, generated from decompression of high density amorphous ice (HDA),[38] does not resemble supercooled water's structure beyond the first two shells, which is a liquid with large fractions of LDL-like structures at these low temperatures. LDA seems to have instead more connection with hexagonal ice, although far from perfect, as seen in Fig. 5. This comparison could imply that LDA contains a large number of small nuclei of hexagonal ice, consisting of six-member rings but lacking enough repeating unit cells to give sharp and detectable Bragg reflections in x-ray scattering as well as sharper features around g_4 and g_5. The low temperature during the LDA preparation prevents growth of the ice nuclei into larger ice crystallites. It is only when the temperature of LDA has been increased to 150 K that crystallization is observed[54] through the appearance of Bragg peaks due to an increase in diffusion and crystal growth. The question is if LDA prepared by hyper quenching of the liquid[55] would give r_5 closer to water at 234.8 K. Such a measurement could eventually more firmly establish the connection between LDA and water.

Clearly, r_4 and r_5 in supercooled water show little resemblance to the units of 6-member rings that build up hexagonal ice.[25] It is also quite remarkable how narrow the peaks in water are in comparison with the condensed solids in Fig. 5. There must be some rather well-defined structural units that build up the LDL configurations. It has been suggested, based on simulations, that there are pentamer rings of water molecules that exist transiently in liquid water.[12,56–58] The fused structures of such a pentamer form of liquid[57] and their concentration increase as the temperature is decreased.[12,58] Clathrate hydrates consist of cagelike structures, where such fused structures are found. Specifically, a dodecahedron consisting of 20 water molecules and 12 pentagonal faces is a primary
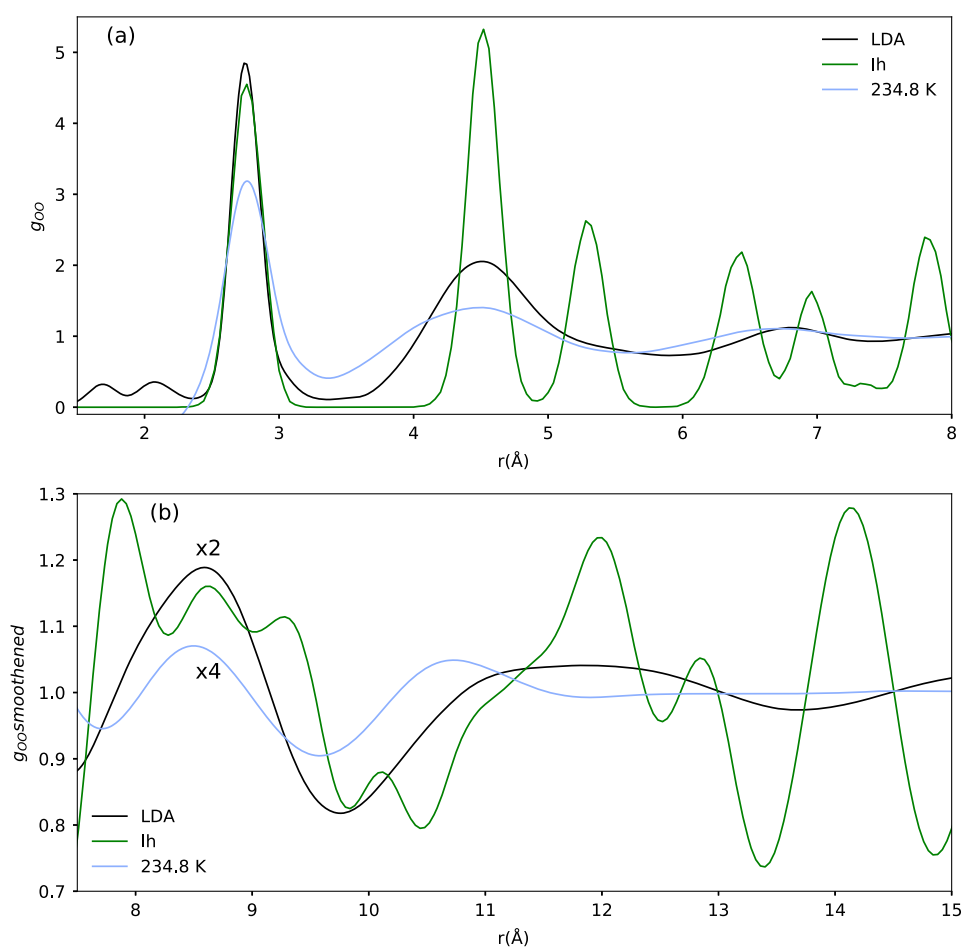
FIG. 5. (a) A comparison of $g_{OO}(r)$ for LDA,[38] hexagonal ice[38] and water at 234.8 K at r < 8 Å. (b) Smoothened $g_{OO}(r)$ is shown for 7.5 < r (Å) < 15. PDF for 234.8 K water is smoothened and is multiplied by 4 and offset by 3, and PDF for LDA is multiplied by 2 and offset by 1, respectively, for better comparison. The smoothening parameters are the same as used in Fig. 2(b).

hydrate structure. The O–H stretch Raman spectra of supercooled water also resemble that of clathrate hydrates.[59] The circumscribed sphere of a regular dodecahedron has a diameter of 2.803 × a, where a is the side of the pentagon. If a is assumed to be the distance of the nearest neighbor in O–O (2.8 Å), we get a diameter of the circumscribed sphere of the dodecahedron as 7.85 Å. This distance is close to r_4 of 8.5 Å for our experimental data at 234.8 K. Indeed, recent simulations of dodecahedron structures[60] indicate distances and narrow peaks in the O–O PDF consistent with the experimental results here presented. Following Yokoyama *et al.*[25] we propose that the 4th and 5th peaks in the O–O PDF of water are related to LDL-like 5-member rings and the narrowness indicates that only negligible amounts of 6-member rings exist in supercooled water. The latter can explain why it is relatively easy to supercool water since in order to make an hexagonal ice nucleus, it is necessary to break apart the LDL 5-member rings that may even consist of large pentamer dodecahedron units to form 6-member rings. This structural rearrangement when supercooled water undergoes homogeneous nucleation to form crystalline ice has been seen in molecular dynamics simulations of TIP4P/2005[12,61] and ST2[62] water models.

We note that r_4 and r_5 as a function of temperature shown in Fig. 3 change linearly down to around 250 K below which there is a sudden change in slope or even direction. We know that at temperatures colder than 250 K there is an accelerated growth of tetrahedral structures,[8,9] and if these are incorporated into larger building units of dodecahedron structures, there can be a rapid contraction of the distances as the collective vibrational motion slows down. Therefore, it is possible that there could be an essential change in the collective behavior of water around 250 K toward lower temperature. It will be essential in the future if this is seen in other measurements, and with the development of XFEL experiments, it may become possible to also conduct single shot x-ray scattering measurements of micrometer sized water droplets out to large Q down to temperatures around 227 K and see if this trend of more rapid changes of distances continues or becomes even more accelerated.

IV. CONCLUSIONS

We have measured the structure factor of liquid water at 5 different supercooled temperatures down to 234.8 K over a wide

Q-range and calculated the O–O PDF up to the fifth shell. We observe that the peak height for the 4th and 5th shells in the PDF (g_4 and g_5) increases on supercooling. We also observe that the peak location of the 4th peak (r_4) shifts to shorter distances on supercooling consistent with an increase in LDL-like structures. This shift is accelerated at temperatures less than 250 K. The 5th peak position (r_5), contrastingly, remains relatively constant or shifts mildly to longer distances on cooling for temperatures hotter than 250 K. For temperatures below 250 K, this trend is reversed and the peak shifts to slightly shorter distances on cooling.

The O–O running coordination number (n_{OO}) suggests an isosbestic point at $r_{iso} = 3.31 \pm 0.05$ Å with n_{OO} of 4.39 ± 0.15. This observation of an isosbestic point over a wide range of temperatures from 366 K to 235 K suggests that the 4-coordination of water is conserved on heating where the molecules shift to slightly longer distances but shorter than r_{iso} and most likely also bend at angles different from the tetrahedral structure. Comparison of the intermediate range O–O correlations of our coldest water at 235 K with LDA and hexagonal ice shows a stark contrast from the third shell onwards at r ≈ 6.7 Å, indicating that the long-range structures in supercooled water are distinctly different than that present in LDA or hexagonal ice. We propose that the LDL-like structures in water may consist of pentamer rings.

SUPPLEMENTARY MATERIAL

See supplementary material for the measured $S_{OO}(Q)$ and the calculated $g_{OO}(r)$. The effect of Q_{max} and dS_{OH}/dT on the calculated O–O PDF is also shown.

ACKNOWLEDGMENTS

REFERENCES

[1] M. F. Chaplin, http://www1.lsbu.ac.uk/water/index.html, 2019.

[2] O. Mishima and H. E. Stanley, Nature **396**, 329 (1998).

[3] P. G. Debenedetti, J. Phys.: Condens. Matter **15**, R1669 (2003).

[4] A. Nilsson and L. G. M. Pettersson, Nat. Commun. **6**, 8998 (2015).

[5] H. E. Stanley, S. V. Buldyrev, O. Mishima, M. R. Sadr-Lahijany, A. Scala, and F. W. Starr, J. Phys.: Condens. Matter **12**, A403 (2000).

[6] P. Gallo, K. Amann-Winkel, C. A. Angell, M. A. Anisimov, F. Caupin, C. Chakravarty, E. Lascaris, T. Loerting, A. Z. Panagiotopoulos, and J. Russo, Chem. Rev. **116**, 7463 (2016).

[7] R. J. Speedy and C. A. Angell, J. Chem. Phys. **65**, 851 (1976).

[8] K. H. Kim, A. Späh, H. Pathak, F. Perakis, D. Mariedahl, K. Amann-Winkel, J. A. Sellberg, J. H. Lee, S. Kim, J. Park, K. H. Nam, T. Katayama, and A. Nilsson, Science **358**, 1589 (2017).

[9] J. A. Sellberg, C. Huang, T. A. McQueen, N. D. Loh, H. Laksmono, D. Schlesinger, R. G. Sierra, D. Nordlund, C. Y. Hampton, D. Starodub, D. P. DePonte, M. Beye, C. Chen, A. V. Martin, A. Barty, K. T. Wikfeldt, T. M. Weiss, C. Caronna, J. Feldkamp, L. B. Skinner, M. M. Seibert, M. Messerschmidt, G. J. Williams, S. Boutet, L. G. M. Pettersson, M. J. Bogan, and A. Nilsson, Nature **510**, 381 (2014).

[10] V. Holten and M. A. Anisimov, Sci. Rep. **2**, 713 (2012).

[11] Y. Liu, J. C. Palmer, A. Z. Panagiotopoulos, and P. G. Debenedetti, J. Chem. Phys. **137**, 214505 (2012).

[12] J. Russo and H. Tanaka, Nat. Commun. **5**, 3556 (2014).

[13] P. H. Poole, F. Sciortino, U. Essmann, and H. E. Stanley, Nature **360**, 324 (1992).

[14] G. A. Appignanesi, J. A. Rodriguez Friz, and F. Sciortino, Eur. Phys. J. E **29**, 305 (2009).

[15] K. T. Wikfeldt, A. Nilsson, and L. G. M. Pettersson, Phys. Chem. Chem. Phys. **13**, 19918 (2011).

[16] L. G. M. Pettersson and A. Nilsson, J. Non-Cryst. Solids **407**, 399 (2015).

[17] H. Pathak, J. C. Palmer, D. Schlesinger, K. T. Wikfeldt, J. A. Sellberg, L. G. M. Pettersson, and A. Nilsson, J. Chem. Phys. **145**, 134507 (2016).

[18] A. K. Soper and M. A. Ricci, Phys. Rev. Lett. **84**, 2881 (2000).

[19] C. Huang, K. T. Wikfeldt, T. Tokushima, D. Nordlund, Y. Harada, U. Bergmann, M. Niebuhr, T. M. Weiss, Y. Horikawa, M. Leetmaa, M. P. Ljungberg, O. Takahashi, A. Lenz, L. Ojamäe, A. P. Lyubartsev, S. Shin, L. G. M. Pettersson, and A. Nilsson, Proc. Natl. Acad. Sci. U. S. A. **106**, 15214 (2009).

[20] A. H. Narten, M. D. Danford, and H. A. Levy, Discuss. Faraday Soc. **43**, 97 (1967).

[21] J. Morgan and B. E. Warren, J. Chem. Phys. **6**, 666 (1938).

[22] A. V. Okhulkov, Y. N. Demianets, and Y. E. Gorbaty, J. Chem. Phys. **100**, 1578 (1994).

[23] G. Hura, J. M. Sorenson, R. M. Glaeser, and T. Head-Gordon, J. Chem. Phys. **113**, 9140 (2000).

[24] B. Tomberli, C. J. Benmore, P. A. Egelstaff, J. Neuefeind, and V. Honkimäki, J. Phys.: Condens. Matter **12**, 2597 (2000).

[25] H. Yokoyama, M. Kannami, and H. Kanno, Chem. Phys. Lett. **463**, 99 (2008).

[26] J. Neuefeind, C. J. Benmore, J. K. R. Weber, and D. Paschek, Mol. Phys. **109**, 279 (2011).

[27] L. B. Skinner, C. Huang, D. Schlesinger, L. G. M. Pettersson, A. Nilsson, and C. J. Benmore, J. Chem. Phys. **138**, 074506 (2013).

[28] C. Benmore, L. C. Gallington, and E. Soignard, "Intermediate range order in supercooled water," Mol. Phys. (published online 2019).

[29] L. B. Skinner, C. J. Benmore, and J. B. Parise, Nucl. Instrum. Methods Phys. Res., Sect. A **662**, 61 (2012).

[30] C. Huang, K. T. Wikfeldt, D. Nordlund, U. Bergmann, T. McQueen, J. Sellberg, L. G. M. Pettersson, and A. Nilsson, Phys. Chem. Chem. Phys. **13**, 19997 (2011).

[31] J. L. F. Abascal and C. Vega, J. Chem. Phys. **123**, 234505 (2005).

[32] E. Shiratani and M. Sasai, J. Chem. Phys. **104**, 7671 (1996).

[33] E. Shiratani and M. Sasai, J. Chem. Phys. **108**, 3264 (1998).

[34] D. Schlesinger, K. T. Wikfeldt, L. B. Skinner, C. J. Benmore, A. Nilsson, and L. G. M. Pettersson, J. Chem. Phys. **145**, 084503 (2016).

[35] L. B. Skinner, C. J. Benmore, J. C. Neuefeind, and J. B. Parise, J. Chem. Phys. **141**, 214507 (2014).

[36] S. D. Overduin and G. N. Patey, J. Phys. Chem. B **116**, 12014–12020 (2012).

[37] A. Perera, Mol. Phys. **109**, 2433 (2011).

[38] D. Mariedahl, F. Perakis, A. Späh, H. Pathak, K. H. Kim, G. Camisasca, D. Schlesinger, C. Benmore, L. G. M. Pettersson, A. Nilsson, and K. Amann-Winkel, J. Phys. Chem. B **122**, 7616 (2018).

[39] B. Henrich, A. Bergamaschi, C. Broennimann, R. Dinapoli, E. F. Eikenberry, I. Johnson, M. Kobas, P. Kraft, A. Mozzanica, and B. Schmitt, Nucl. Instrum. Methods Phys. Res., Sect. A **607**, 247 (2009).

[40] P. Kraft, A. Bergamaschi, C. Broennimann, R. Dinapoli, E. F. Eikenberry, B. Henrich, I. Johnson, A. Mozzanica, C. M. Schlepütz, P. R. Willmott, and B. Schmitt, J. Synchrotron Radiat. **16**, 368 (2009).

[41] M. Knudsen, Ann. Phys. **352**, 697 (1915).

[42] C. Goy, M. A. C. Potenza, S. Dedera, M. Tomut, E. Guillerm, A. Kalinin, K.-O. Voss, A. Schottelius, N. Petridis, A. Prosvetov, G. Tejeda, J. M. Fernández,

C. Trautmann, F. Caupin, U. Glasmacher, and R. E. Grisenti, Phys. Rev. Lett. **120**, 015501 (2018).

[43] D. Schlesinger, J. A. Sellberg, A. Nilsson, and L. G. M. Pettersson, J. Chem. Phys. **144**, 124502 (2016).

[44] A. P. Hammersley, S. O. Svensson, M. Hanfland, A. N. Fitch, and D. Hausermann, High Pressure Res. **14**, 235 (1996).

[45] A. Savitzky and M. J. E. Golay, Anal. Chem. **36**, 1627 (1964).

[46] J. Wang, A. N. Tripathi, and V. H. Smith, J. Chem. Phys. **101**, 4842 (1994).

[47] Z. Su and P. Coppens, Acta Crystallogr., Sect. A: Found. Crystallogr. **54**, 357 (1998).

[48] A. K. Soper, J. Phys.: Condens. Matter **19**, 335206 (2007).

[49] K. T. Wikfeldt, M. Leetmaa, M. P. Ljungberg, A. Nilsson, and L. G. M. Pettersson, J. Phys. Chem. B **113**, 6246 (2009).

[50] A. K. Soper and E. R. Barney, J. Appl. Crystallogr. **45**, 1314 (2012).

[51] J. Waser and V. Schomaker, Rev. Mod. Phys. **25**, 671 (1953).

[52] G. Camisasca, H. Pathak, K. T. Wikfeldt, and L. G. M. Pettersson, "Radial distribution functions of water: models vs experiments," J. Chem. Phys. (submitted).

[53] P. Wernet, D. Nordlund, U. Bergmann, M. Cavalleri, M. Odelius, H. Ogasawara, L. Å. Näslund, T. K. Hirsch, L. Ojamäe, P. Glatzel, L. G. M. Pettersson, and A. Nilsson, Science **304**, 995 (2004).

[54] K. Amann-Winkel, C. Gainaru, P. H. Handle, M. Seidl, H. Nelson, R. Böhmer, and T. Loerting, Proc. Natl. Acad. Sci. U. S. A. **110**, 17720 (2013).

[55] E. Mayer, J. Appl. Phys. **58**, 663 (1985).

[56] R. J. Speedy, J. Phys. Chem. **88**, 3364 (1984).

[57] M. Mandziuk, J. Mol. Struct. **1177**, 168 (2019).

[58] B. Santra, R. A. DiStasio, F. Martelli, and R. Car, Mol. Phys. **113**, 2829 (2015).

[59] G. E. Walrafen, W. H. Yang, and Y. C. Chu, *Supercooled Liquids* (American Chemical Society, 1997), p. 287.

[60] G. Camisasca, D. Schlesinger, I. Zhovtobriukh, G. Pitsevich, and L. G. M. Pettersson, "A Proposal for the Structure of High- and Low-Density Fluctuations in Liquid Water," J. Chem. Phys. (submitted).

[61] M. Matsumoto, S. Saito, and I. Ohmine, Nature **416**, 409 (2002).

[62] J. C. Palmer, F. Martelli, Y. Liu, R. Car, A. Z. Panagiotopoulos, and P. G. Debenedetti, Nature **510**, 385 (2014).